Interferometric identification of surface-related multiples

Boullenger, Boris; Draganov, Deyan

Important note
To cite this publication, please use the final published version (if applicable).
Please check the document version above.

Interferometric identification of surface-related multiples

Boris Boullenger[1] and Deyan Draganov[1]

ABSTRACT

The theory of seismic interferometry predicts that crosscorrelations of recorded seismic responses at two receivers yield an estimate of the interreceiver seismic response. The interferometric process applied to surface-reflection data involves the summation, over sources, of crosscorrelated traces, and it allows retrieval of an estimate of the interreceiver reflection response. In particular, the crosscorrelations of the data with surface-related multiples in the data produce the retrieval of pseudophysical reflections (virtual events with the same kinematics as physical reflections in the original data). Thus, retrieved pseudophysical reflections can provide feedback information about the surface multiples. From this perspective, we have developed a data-driven interferometric method to detect and predict the arrival times of surface-related multiples in recorded reflection data using the retrieval of virtual data as diagnosis. The identification of the surface multiples is based on the estimation of source positions in the stationary-phase regions of the retrieved pseudophysical reflections, thus not necessarily requiring sources and receivers on the same grid. We have evaluated the method of interferometric identification with a two-layer acoustic example and tested it on a more complex synthetic data set. The results determined that we are able to identify the prominent surface multiples in a large range of the reflection data. Although missing near offsets proved to cause major problems in multiple-prediction schemes based on convolutions and inversions, missing near offsets does not impede our method from identifying surface multiples. Such interferometric diagnosis could be used to control the effectiveness of conventional multiple-removal schemes, such as adaptive subtraction of multiples predicted by convolution of the data.

INTRODUCTION

In conventional reflection surveys, seismic measurements are acquired at or near the earth's surface, resulting in the presence of surface-related multiple reflections. The surface-related multiples are caused by waves bouncing once or several times at the earth's free surface. Yet, most of the current imaging algorithms assume that the reflection data consist only of primary events, that is, seismic waves that have reflected only once in the subsurface before being recorded. Thus, these algorithms associate the multiple reflections with noise. Therefore, the multiple reflections need to be suppressed from the recorded reflection data to avoid being misinterpreted as actual reflectors during the geologic interpretation. The presence of strong surface-related multiples is a well-identified problem in marine seismic data (Yilmaz, 1987). Free-surface multiples can also be significant in land seismic data, but they are less often easily identified due to the complex nature of the near surface as well as, in general, more irregular acquisition geometries (Kelamis and Verschuur, 2000).

Multiple-suppression methods can be classified in two categories. The first category includes methods exploiting the differential spatial behavior (moveout) between multiples and primaries, for example, via Radon transforms (Hampson, 1986; Trad, 2003). The separation of multiples by filtering will fail when the multiples have moveouts similar to the primaries, a property that often occurs at near offsets. The second category of methods exploits the predictability of the multiples. Surface multiples can be predicted by multidimensional convolutions of the reflection data and then eliminated by, for example, adaptive subtraction (Verschuur et al., 1992; Berkhout and Verschuur, 1997). For corresponding schemes, the data often need to be regularized to data with source and receiver positions on the same grid. In addition, not having the near offsets, as is common in marine data, may affect the prediction of the surface multiples within a large range of the data.

Although surface-related multiples are undesirable in conventional seismic imaging, they prove to be useful signals in controlled-source applications of seismic interferometry. Seismic interferometry, as a theory, refers to the principle of estimating an interreceiver seismic response by crosscorrelating the measured responses at the same two receivers. This principle forms the basis for noise-correlation seismology (Campillo and Paul, 2003; Sabra et al., 2005; Draganov et al., 2009; Ruigrok and Wapenaar, 2012; Boullenger et al., 2015). With controlled sources, the retrieved interreceiver response can be obtained by crosscorrelation of the individual source responses and summation over the sources. This interferometric technique leads to several applications in exploration seismology, such as interferometric redatuming below a complex overburden (Bakulin and Calvert, 2006) or refraction-signal enhancement (Bharadwaj et al., 2012). A review of the possible interferometric methods could be found in Schuster (2009).

When applied to surface reflection data, seismic interferometry allows the retrieval of estimates of the interreceiver reflection responses, as if from a source at one of the receiver positions (Schuster et al., 2004). The new source position is referred to as a virtual-source position. The repetition of the crosscorrelation and summation process for different receiver pairs allows turning the receivers into virtual sources and the original reflection data into virtual reflection data. The crosscorrelation of different orders of surface multiples (including primaries with multiples) retrieves pseudoprimaries and lower order multiples. Such pseudophysical reflections exhibit kinematics coinciding with those of physical reflections in the original reflection data. The term "pseudo" is used to qualify these retrieved events because the amplitudes are not directly comparable with, and the wavelet is different from, the corresponding events in the original data (Löer et al., 2013). Consequently, the retrieved pseudophysical reflections are indicators of the presence of the surface-related multiples in the reflection data and thus may be exploited for identification of the multiples.

Multiple suppressions based on crosscorrelation of the data were proposed by Berkhout and Verschuur (2006) using the so-called focal transform formalism. Because the design of the focal-transform operator requires a good prior estimate of the primaries, the method is introduced only in association with conventional multiple prediction using convolutions. Later, van Groenstijn and Verschuur (2009)

use crosscorrelations to develop an iterative algorithm of estimation of primaries by sparse inversion. By imposing an additional sparsity constraint, they overcome limitations from direct-inversion methods (van Borselen et al., 1996). However, the inversion problem still requires regularly sampled data with sources and receivers on the same grid.

In this paper, we introduce a method to detect and identify surface-related multiple reflections by predicting their arrival times for multiple source-receiver pairs. The method is based on the study of retrieved pseudoreflections in virtual data obtained by applying the principles of seismic interferometry to surface-controlled sources. As the interferometric diagnosis is conducted independently for any pair of receivers, the method does not require regularly sampled receivers, it does not require the receivers to coincide with source positions either. First, we review the principle of reflected-wave seismic interferometry with controlled sources and discuss how crosscorrelation exploits the multiple reflections to yield pseudophysical reflections in the virtual data. Through an illustrative example based on a layer-cake model, we show that multiple energy can be detected by stationary-phase analysis of the retrieved pseudophysical reflections. As an investigation of the advantages and limitations, we also test the method on a modified version of the Sigsbee 2B acoustic model.

REFLECTED-WAVE SEISMIC INTERFEROMETRY WITH CONTROLLED SOURCES

Mathematical representations of seismic interferometry are based on Rayleigh's reciprocity theorems (Claerbout, 1976; Wapenaar, 2004; Schuster and Zhou, 2006). A generalization of the theory to 3D elastodynamic media is derived by Wapenaar and Fokkema (2006). They consider two receivers, positioned at $\mathbf{x}_A$ and $\mathbf{x}_B$, embedded in a lossless inhomogeneous medium, and enclosed by a sufficiently large surface of sources S (Figure 1a). In the acoustic situation, the retrieval of the interreceiver Green's function is given by the seismic-interferometry relation:

$$G(\mathbf{x}_B, \mathbf{x}_A, t) + G(\mathbf{x}_A, \mathbf{x}_B, -t)$$
$$\propto \oint_S \{G(\mathbf{x}_B, \mathbf{x}, t) \otimes G(\mathbf{x}_A, \mathbf{x}, -t)\} d^2\mathbf{x}, \qquad (1)$$

where $\otimes$ denotes convolution and $\mathbf{x}$ is the source coordinate along S. The Green's function $G(\mathbf{x}_B, \mathbf{x}_A, t)$ is the monopole response at the receiver at $\mathbf{x}_B$ from an impulsive monopole source at $\mathbf{x}_A$. Here, $G(\mathbf{x}_A, \mathbf{x}_B, -t)$ is the acausal version of $G(\mathbf{x}_B, \mathbf{x}_A, t)$ (after using source-receiver reciprocity) and is defined only at negative time lags. From equation 1, seismic interferometry predicts that the seismic response from $\mathbf{x}_A$, the virtual-source position, to $\mathbf{x}_B$ can be estimated by crosscorrelating individual responses recorded at the two receivers from each of the sources on S and integrating over the sources. This relation includes far-field and high-frequency approximations to circumvent the need of dipole-source measurements and assumes the medium parameters to be homogeneous outside S as well as smoothly varying across S.

In seismic exploration, the acquisition geometry most often involves receivers deployed at the earth's free surface. As depicted in Figure 1b, seismic sources are required only along the semisphere S_1 below the receivers, which becomes the only remaining integration surface in equation 1 (Wapenaar and Fokkema, 2006). Very often, though, the seismic sources are only active at the same surface S_0 in which the
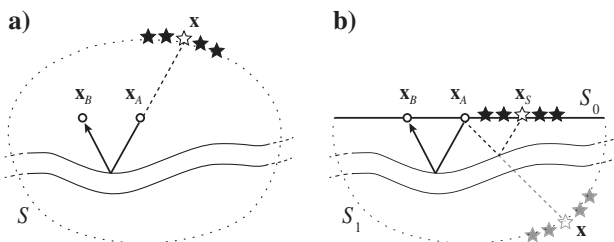

Figure 1. Interferometric retrieval of an interreceiver reflection arrival from $\mathbf{x}_A$ (virtual-source position) to $\mathbf{x}_B$. (a) Required configuration with a surface S of sources enclosing the receivers. The white star at $\mathbf{x}$ on S indicates the source at the stationary-phase point: the wave passing through $\mathbf{x}_A$ shares the same interreceiver raypath as the reflection event from a virtual source at $\mathbf{x}_A$. (b) Actual configuration in seismic exploration: The sources and receivers are at the earth's free surface S_0. The white star $\mathbf{x}_S$ indicates a secondary stationary-phase source position, which partly shares a common travel path with the ray from the theoretically required stationary-phase source position at $\mathbf{x}$ on S_1.

receivers are placed. This means that an integration can be carried out only along S_0, along which sources are actually not required. However, the wavefields generated by surface sources contain raypaths, between the positions $\mathbf{x}_A$ and $\mathbf{x}_B$, coinciding with those of wavefields generated by subsurface sources. For example, in Figure 1b, the source at $\mathbf{x}_S$ on S_0 contributes to the estimate of the same interreceiver reflection arrival as the source at $\mathbf{x}$ on S_1. In this example, $\mathbf{x}$ is referred to as a (primary) stationary-phase position for the retrieval of the primary reflection between $\mathbf{x}_A$ and $\mathbf{x}_B$, whereas $\mathbf{x}_S$ is referred to as a secondary stationary-phase position (as a result of being a projection to the surface of position $\mathbf{x}$). From Figure 1b, we see that the crosscorrelation of the primary reflection at $\mathbf{x}_A$ from $\mathbf{x}_S$ with its first-order free-surface multiple at $\mathbf{x}_B$ retrieves a (pseudo) primary reflection between $\mathbf{x}_A$ and $\mathbf{x}_B$ (Halliday et al. [2007]; see also van Wijk [2006] for a laboratory-data example from one-layer sample). In practice, the existence of at least one secondary stationary-phase source will be limited only by the aperture of the surface-source array. Note that, for convenience, in what follows, we will omit the adjective secondary.

Although the surface-source acquisition geometry does not comply with the theoretically required subsurface-source distribution, applying seismic-interferometry principles via integration over sources only at the free surface will still provide an estimate of the interreceiver Green's function. For one-sided illumination with source and receivers at the surface, we define the retrieved virtual reflection data estimate as

$$C(\mathbf{x}_B, \mathbf{x}_A, t) = \sum_{S_0} \{R(\mathbf{x}_B, \mathbf{x}_S, t) \otimes R(\mathbf{x}_A, \mathbf{x}_S, -t)\} d^2\mathbf{x}_S, \quad (2)$$

where $\mathbf{x}_A$ and $\mathbf{x}_B$ are the two receiver positions, and R denotes the reflection response. The integration over S in equation 1 is replaced, in equation 2, by a discrete summation over S_0 of individual crosscorrelations of the reflection responses at $\mathbf{x}_A$ and $\mathbf{x}_B$. The constructive summation in the vicinity of stationary-phase positions (Snieder, 2004) yields estimates of pseudophysical reflections, i.e., events with kinematics as of actual reflections. However, the absence of subsurface sources (integration only over S_0) will also give rise to nonphysical (or ghost) reflection events. These retrieved spurious reflections are observed and discussed by several authors, such as Snieder et al. (2006), King and Curtis (2012), Draganov et al. (2012), or Boullenger et al. (2014). As a result, we now have a correlation function C, instead of the interreceiver Green's functions between $\mathbf{x}_A$ and $\mathbf{x}_B$; this result also contains spurious events, including nonphysical reflections.

Note, that in the presence of refracted waves, another type of spurious energy, so-called virtual refractions, would be retrieved as the result of the crosscorrelation of those waves (Dong et al., 2006; Mikesell et al., 2009).

IDENTIFICATION OF SURFACE MULTIPLES

Figure 2 illustrates the interferometric retrieval of pseudophysical reflections in the case of two

reflectors in the subsurface and sources at the surface, i.e., using secondary stationary-phase sources. Two receivers are positioned at the earth's free surface, at $\mathbf{x}_A$ and $\mathbf{x}_B$, respectively. We consider the reflection responses from sources along the free surface, containing primary reflections (including internal multiples) as well as surface-related multiples (or simply surface multiples). As we apply equation 2 to the reflection data, the recorded reflection events at $\mathbf{x}_A$ and $\mathbf{x}_B$ are all crosscorrelated, resulting in retrieved pseudophysical reflections as well as nonphysical arrivals.

As indicated in Figure 2a with travel paths from a source in a stationary-phase region, the crosscorrelation of the first primary event at $\mathbf{x}_A$ with its first-order surface multiple at $\mathbf{x}_B$ contributes to the retrieval of the first pseudoprimary arrival from a virtual source at $\mathbf{x}_A$. Other contributions to this retrieved pseudophysical event will come, for example, from the crosscorrelation of the first-order surface multiple at $\mathbf{x}_A$ with the second-order surface multiple at $\mathbf{x}_B$ (Figure 2b), or of the second primary event at $\mathbf{x}_A$ with its first-order surface multiple at $\mathbf{x}_B$ (Figure 2c).

The role played by the surface multiples in the retrieval of a first pseudoprimary arrival can be extended to any retrieved pseudoprimary reflection. Figure 2d shows that the retrieved second pseudoprimary reflection would result from the crosscorrelation of the first primary event at $\mathbf{x}_A$ with its first-order surface multiple at $\mathbf{x}_B$, but also from the crosscorrelation of the first-order surface multiple with a second-order surface multiple (Figure 2e), and of the second primary with its first-order surface multiple (Figure 2f).

In addition, the crosscorrelation of surface multiples of different orders allows the retrieval of pseudophysical multiples. Figure 2g illustrates how the pseudo first-order surface multiple would be retrieved from the crosscorrelation of the first primary at $\mathbf{x}_A$ with its second-order surface multiple at $\mathbf{x}_B$, second-order surface multiple with the third-order surface multiple (Figure 2h), and second primary with its second-order surface multiple (Figure 2i).
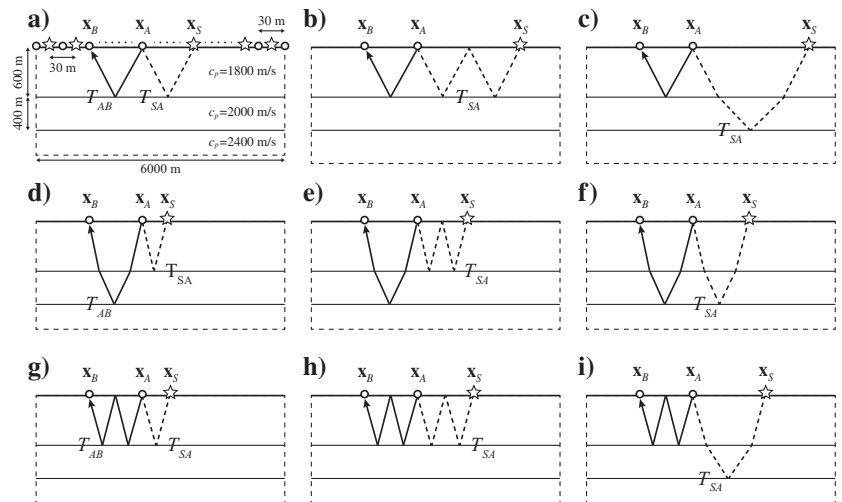

Figure 2. Contributions of surface multiples to retrieved pseudophysical reflections between receivers at $\mathbf{x}_A$ and $\mathbf{x}_B$. The white stars indicate stationary-phase source positions $\mathbf{x}_S$ for the retrieved events. (a-c) The retrieved event is the pseudoprimary reflection from the first reflector. (d-f) The pseudoprimary reflection from the second reflector. (g-i) Contributions to a retrieved (pseudo-) first-order surface multiple. Here, T_{SA} and T_{AB} are the traveltimes along the illustrated reflected travel paths from $\mathbf{x}_S$ and $\mathbf{x}_A$, and from $\mathbf{x}_A$ and $\mathbf{x}_B$, respectively.

The presence of surface-related multiples in the reflection data translates into retrieved pseudophysical reflections in the virtual data. These virtual reflection events exhibit the same kinematics as physical reflections in the original data, hence the use of the term pseudo. In general, the crosscorrelation between an nth-order surface multiple ($n = 0$ defining primary reflections) at $\mathbf{x}_A$ and an mth-order surface multiple at x_B ($m > n \geq 0$) contributes to the retrieval of the pseudo ($m - n - 1$)th-order surface multiple in the interferometric results. Therefore, retrieved pseudophysical reflection events are evidences of the presence of significant surface multiples in the original data. Additional information about the contributing surface multiples can be obtained with stationary-phase analysis of the retrieved events.

The study of how pseudophysical reflections are retrieved forms the basis of the proposed interferometric identification of surface multiples. The first step is the detection of pseudophysical reflections retrieved using seismic interferometry. This can be done by selecting a (significant) reflection event in the data (it can be any primary or multiple reflection, including internal multiples), and checking if there is a kinematically equivalent event retrieved in the virtual data. The detection of pseudophysical reflections indicates that contributing surface-related multiples are present in the data. The retrieval time T_{AB} of such an event for a virtual source at $\mathbf{x}_A$ and a receiver at $\mathbf{x}_B$ is the traveltime, from $\mathbf{x}_A$, of waves recorded as surface multiples at $\mathbf{x}_B$ (Figure 2).

As formulated in equation 2, the retrieved pseudophysical reflection at T_{AB} results from interreceiver crosscorrelation and stacking over sources. Constructive summation takes place for adjacent sources in the stationary-phase regions. For such a stationary-phase source, the recorded wavefield at $\mathbf{x}_B$ has first propagated to $\mathbf{x}_A$ where it is recorded as a primary or surface multiple reflection with an arrival time T_{SA}. In turn, this wavefield is recorded as a higher order surface multiple at $\mathbf{x}_B$. For identified stationary-phase sources, such as those represented at positions $\mathbf{x}_S$ in Figure 2, the arrival time of the surface multiples recorded at $\mathbf{x}_B$ can be estimated by adding the traveltime T_{SA} and the retrieval time T_{AB}.

In accordance with the above explanation, the key steps of the interferometric identification of surface multiples are the detection of retrieved pseudophysical reflections (providing T_{AB}) and their corresponding stationary-phase sources (providing T_{SA}). The latter is done by analyzing the individual crosscorrelated responses. Because the arrival times of the surface multiples can be estimated only for some retrieved pseudophysical events and for some source positions, our method does not allow predicting the multiples in an entire gather, nor to predict all multiples. However, the method allows identifying prominent surface multiples for the detected stationary-phase sources. By repeating the above scheme for multiple pairs of receivers, one can estimate the arrival times of several surface multiples in the reflection data for a large receiver range. This is illustrated, together with the stationary-phase analysis, in the example below.

ILLUSTRATIVE EXAMPLE

We illustrate the method with a simple numerical acoustic example using the velocity model and the source-receiver geometry in Figure 2a. The fixed receiver positions range from 0 to 6000 m, the sources are placed between the receivers, from 15 to 5985 m. The receivers and sources are regularly sampled with 30 m spacing. The modeled reflection data contain primary reflections (including weak internal multiples) and several surface-related multiples due to the free surface. Figure 3a shows the modeled common-receiver gather for the position $x_B = 2400$ m. Note that, as prescribed in equation 2, the direct waves are suppressed because they would otherwise interfere in the crosscorrelation and damage the retrieval of pseudophysical reflections.

We retrieve the virtual reflection data using equation 2, with virtual sources at every receiver position. Figure 3b shows the resulting (virtual) common-receiver gather for the position $x_B = 2400$ m. The gather is dominated at earlier times by artifacts (arrow 2 indicating a finite-aperture artifact, even though the edge sources in the gathers were tapered for the summation) and a strong nonphysical (ghost) reflection (arrow 3). However, we may already visually recognize several retrieved pseudoreflections sharing the same kinematics as the physical reflections in the gather in Figure 3a.

The first step toward the identification of surface multiples is the detection of retrieved pseudophysical reflections. To this end, we select the traveltime curve of an arbitrary reflection event in the receiver gather from the original reflection data (dashed white curve in Figure 3a). Then, we examine if the corresponding pseudoreflection is retrieved in the virtual gather in Figure 3b. This diagnosis may be performed, for example, by estimating a signal-to-noise ratio along the traveltime curve projected in the virtual gather and check that a threshold value is exceeded. For this, we have taken the ratio of the energy, within a time window centered along the traveltime curve, to the energy around that window. The size of the time window corresponds to one period of the reflection signals. If the ratio is not satisfactory, the reflection is considered not retrieved and we choose another reflection in the original data. In case the ratio exceeds the threshold, the event is considered retrieved. Figure 3c shows the detected pseudoreflection event. For illustrative purposes, this event was isolated within the gather. The next step
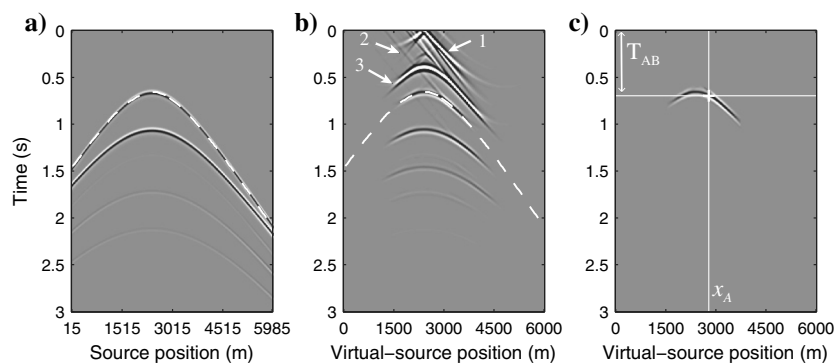

Figure 3. (a) Common-receiver gather for the position $x_B = 2400$ m from the reflection data. The dashed white curve indicates the selected traveltime curve along the first primary reflection. (b) As in (a), but for the retrieved pseudoreflection data. The traveltime curve is repeated from the selection in (a). The white arrows indicate a branch of (1) the smeared delta function, (2) a finite-aperture artifact, and (3) a retrieved nonphysical reflection. (c) The detected pseudoreflection from (b) with mute applied. The solid white lines indicate the selected virtual-source position $x_A = 2790$ m and arrival time T_{AB}.

is the selection of a virtual-source position x_A for this retrieved event, which in turn determines the traveltime T_{AB} of a reflected wave traveling from x_A to x_B. We select the pair $\{x_A, T_{AB}\}$ by picking the detected pseudoreflection in the virtual gather (solid white lines in Figure 3c).

Given the chosen pair of receiver positions, x_B and x_A, we aim to estimate source positions in stationary-phase regions of the retrieved pseudophysical reflection. To this end, we analyze the correlation gather for the correlations between the two receivers (before summation over sources), which is obtained by

$$C_{BA}(x_S, t) = R(x_B, x_S, t) \otimes R(x_A, x_S, -t). \quad (3)$$

In equation 3, C_{BA} is the result of trace-by-trace crosscorrelation of the two common-receiver gathers and, thus, a function of the source position x_S. Figure 4a shows the resulting correlation gather for the receivers at $x_B = 2400$ m and $x_A = 2790$ m. The virtual trace previously selected is actually retrieved by summation of C_{BA} over the source positions. We define this "global" stacked trace as S_G with

$$S_G = \sum_{n=1}^{N_G} C_{BA}[n], \quad (4)$$

where n is the source index and N_G is the total number of sources (traces) in the correlation gathers (here, $N_G = 200$). For the analysis and detection of stationary-phase regions, we also define local (partial) stacks of adjacent traces in the gather C_{BA} as S_P with

$$S_P[ix] = \sum_{n=ix-k}^{ix+k} C_{BA}[n], \quad (5)$$

where ix and n are the source indexes. The number k controls the number of stacked adjacent traces N as $N = 2k + 1$. Note that the edge traces are tapered for the summation. As mentioned in the previous sections, in the vicinity of a stationary-phase position, the summation is constructive and contributes to the retrieved pseudoreflection at T_{AB} (time index iT). For such a source position with index ix^*, the local stacked trace $S_P[ix^*]$ is a stationary-phase approximation of S_G around the retrieved time T_{AB}. To find a prominent stationary-phase source, we calculate the correlation coefficient of $S_P[ix]$ and S_G for the signal retrieved around T_{AB}

$$\gamma[ix] = \frac{\sum_{j=iT-m}^{iT+m} S_P[ix,j] S_G[j]}{\sqrt{\sum_{j=iT-m}^{iT+m} S_P[ix,j]^2} \sqrt{\sum_{j=iT-m}^{iT+m} S_G[j]^2}}, \quad (6)$$

where j is a time index and the number m controls the length of the time window around iT for the correlated retrieved signals. Figure 4b shows the correlation coefficient γ as a function of the source

position x_S. For this example, the stacked traces $S_G[ix]$ are obtained with $N = 21$, which means by stacking 21 adjacent traces. As indicated with a dashed line, the source position for which the correlation coefficient is the highest is $x_{S^*} = 3945$ m. This is the estimated dominant stationary-phase position. We also observe another prominent peak value at approximately $x = 3000$ m, which indicates another stationary-phase region. The existence of at least two important stationary-phase regions can also be shown in Figure 4a, where we can distinguish two correlated events contributing to the same retrieved arrival at around T_{AB}. The graph in Figure 4c shows the estimated position x_{S^*} with respect to the chosen parameter N for the local stacks. For N varying from 11 to 41, we observe a mean estimated position $\{x_{S^*}\}_{av} = 3913$ m and a standard deviation of only 30 m. This result indicates that in this simple numerical example, the estimated position x_{S^*} does not vary significantly with N, and thus,
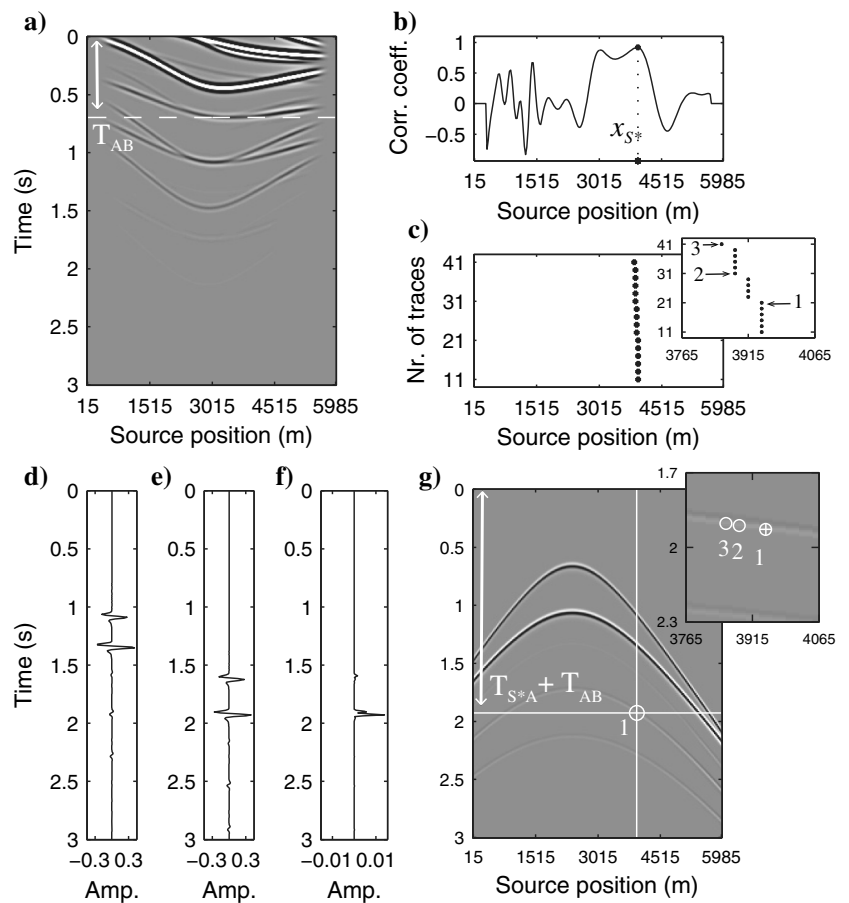

Figure 4. (a) Correlation gather for receivers at $x_B = 2400$ m and $x_A = 2790$ m. (b) Correlation coefficient γ as a function of the source position x_S. The maximum value determines the dominant stationary-phase position $x_{S^*} = 3945$ m. (c) Estimated position x_{S^*} as a function of the number of stacked adjacent traces N in equation 5. The inset shows a magnification of the change of the estimated position. (d) Reflection response at $x_B = 2400$ m from the source at $x_{S^*} = 3945$ m. (e) Time-shifted reflection response at $x_A = 2740$ from the source at $x_{S^*} = 3945$ m: The time shift is equal to the selected retrieval time T_{AB} of the pseudoreflection. (f) Absolute-value result of the sample-by-sample product of the responses in (d and e), used to obtain the traveltime T_{S^*A}. (g) Common-receiver gather at the position $x_B = 2400$ m with predicted arrival time $T_{S^*A} + T_{AB}$ of a surface multiple for the source position (1) $x_{S^*} = 3945$ m. The inset shows a magnification of the identified multiple with also the predicted arrival times for the detected (2) $x_{S^*} = 3885$ and (3) 3855 m using $N = 31$ and 41 in equation 5, respectively.

the stationary-phase analysis is not too sensitive to the choice of N. However, note that sufficient source sampling (two sources per wavelength) is required for the stacking operations.

The position x_{S^*} is detected inside the stationary-phase region of the retrieved pseudoreflection, but it is still undetermined with exactly which of the reflection events recorded at x_A, this stationary-phase region is associated. In other words, it is still unknown at this stage whether the detected position x_{S^*} corresponds to the situation
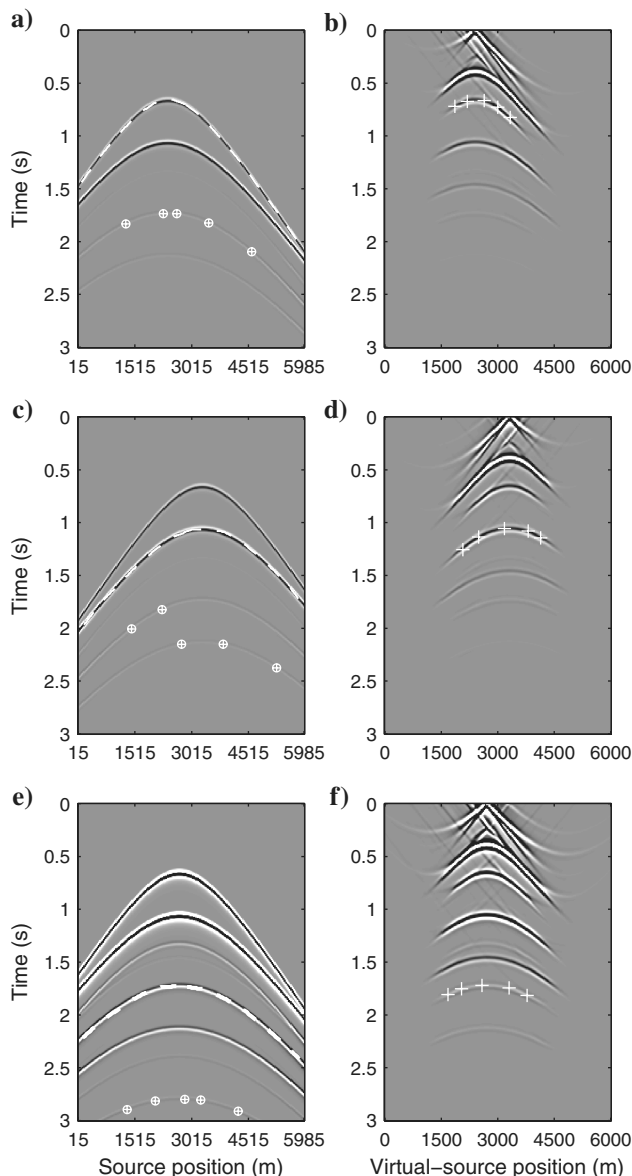

Figure 5. (a) Common-receiver gather at position $x_B = 2400$ m with the selected traveltime curve of a reflection (dashed white curve). (b) Virtual common-receiver gather at position $x_B = 2400$ m. The white crosses indicate the picked virtual-source positions for the detected pseudophysical reflection. The predicted arrival times of surface multiples are indicated with white circles in (a). (c and d) As in (a and b), but for the receiver position $x_B = 3300$ m and a selected traveltime curve corresponding to the second primary reflection. (e and f) The receiver position is $x_B = 2700$ m and the selection corresponds to a first-order surface multiple. For visualization purposes, the panels in (e and f) are clipped to bring forward weaker arrivals.

in Figure 2a, 2b, or 2c, and thus which surface multiple recorded at x_B can be inferred from x_{S^*}. Therefore, we aim to determine the contributing event recorded at x_A, which in turn provides the traveltime T_{S^*A}, the traveltime to the virtual-source position from the estimated stationary-phase source position. Often, especially in the case of marine data, this correlated event will be the first primary reflection. In general, the main contribution will come from the strongest reflection, which is not necessarily, the first primary. The idea is to come back to the crosscorrelation with a time-lag equal to T_{AB}, for which the crosscorrelation produces its maximum contribution to the selected pseudoreflection. Figure 4d shows the recorded reflection response at $x_B = 2400$ m from the source at $x_{S^*} = 3945$ m, and Figure 4e shows the response at x_A from a source at x_{S*} with an additional time-shift equal to T_{AB}. The retrieved pseudophysical reflection at T_{AB} receives contributions from the cross product result of the two traces. The time at which the maximum amplitude is observed indicates the arrival time of the maximum contributor at x_A (Figure 4f). This time can be defined as $T_{S^*A} + T_{AB}$. Thus, T_{S^*A} is obtained by subtracting T_{AB} from it. The predicted arrival time $T_{S^*A} + T_{AB}$ from the source at x_{S^*} to the receiver at x_B is then automatically plotted in the corresponding common-receiver gather (circle with index 1 in Figure 4g). This arrival time coincides with the arrival of a surface-related multiple for that source position.

As mentioned above, the predicted arrival time strongly depends on the estimated stationary position x_{S^*}. In Figure 4c, we observed that the detected x_{S^*} may vary by using different values for the parameter N in the stationary-phase analysis. The magnified panel in Figure 4g shows the resulting predicted arrival times of multiples for two other estimates of $x_{S^*} - x_{S^*} = 3885$ m (index 2) and $x_{S^*} = 3855$ m (index 3), corresponding to $N = 31$ and 41, respectively. In both cases, the predicted arrival times identify the same surface multiple because the detected positions x_{S^*} still belong to the same stationary-phase region.

The above interferometry-based diagnosis may be automatically repeated for several other selected virtual-source positions x_A along the retrieved pseudophysical reflection. This results in predicted arrival times of the multiple for several source positions in the common-receiver gather at $x_B = 2400$ m. Figure 5a and 5b shows the identification of a first-order surface multiple in the gather for five different virtual-source positions. This event corresponds to a first-order multiple of the second primary reflection as represented in Figure 2c, from a first reflection on the second interface. The stationary-phase analysis allowed recognizing the reflection from the second interface as the stronger contributing reflection to the retrieved pseudophysical reflection. This is explained by the fact that the recorded primary reflections on the second interface are stronger than the ones on the first interface.

Figure 5c shows the identification of the first-order multiple of the second primary in the common-receiver gather for another position $x_B = 3300$ m. This time, we select the second primary reflection in the gather. We observe that a retrieved event in the virtual common-receiver gather (Figure 5d) is automatically found to kinematically coincide with the physical reflection. For several virtual-source positions x_A, indicated by white crosses, we predict the dominant stationary-phase source positions and arrival times of multiples indicated by the white circles in Figure 5c.

Note that two different events are intercepted as multiples by the stationary-phase analysis. Due to relatively close amplitude levels between the two primary reflections, the found main contributing

event at x_A is not the same for every virtual-source position, resulting in identifying different multiples. This effect depends on the relative amplitudes of the reflection events in the original data as well as on the parameters defining the local stacking operations that allow estimating the dominant stationary-phase source position.

Finally, we may choose to select any reflection event in the original data including multiple reflections. Figure 5e shows the common-receiver gather for $x_B = 2700$ m and the selection of a first-order surface multiple. A retrieved pseudophysical reflection is automatically detected in the virtual receiver gather in Figure 5f, from which we select several virtual-source positions marked with white crosses. The predicted surface-multiple arrival times are again indicated in Figure 5e. The identified event is a second-order surface multiple.

COMPLEX EXAMPLE

We test the above-described method on a more complex reflection data set, modeled using a slightly modified version of the acoustic Sigsbee 2B model. The Sigsbee 2B model was initially designed to simulate realistic sea-bed multiples and engender salt-imaging challenges. Here, we use the velocity model in Figure 6 together with a constant density model. The fixed-receiver and source positions range from 0 to 10,000 m, with regular 25 and 50 m spacings, respectively. The total simulated recording time is 8 s. Again the modeled direct wave is suppressed to preserve only reflection data.

Figure 7a shows the common-receiver gather for the position $x_B = 4000$ m between 1 and 5 s of two-way traveltime. We apply seismic interferometry to this reflection data using equation 2 for all receiver positions. Therefore, the virtual-source spacing is 25 m. Figure 7b shows the retrieved virtual common-receiver gather for the same receiver position $x_B = 4000$ m. In the reflection data, we select a traveltime curve corresponding to a physical reflection. As indicated by the dashed curve in Figure 7a, this event is in fact the sea-bed primary reflection. A corresponding pseudophysical event is automatically detected in the virtual gather in Figure 7b along the same traveltime curve. This indicates, as expected from the Sigsbee 2B model, that relatively strong surface multiples are present in the reflection data, which contribute to that retrieved event. Note that the retrieved common-receiver gather contains nonphysical reflections as well, but because of the complexity of the model in the lateral direction, these events are not too continuous in the lateral direction and are perceived as "correlation noise." As in the illustrative example, we now choose a virtual-source position ($x_A = 3475$ m), for which the selected event is retrieved well (exceeding an adequate signal-to-noise ratio) and analyze the stationary-phase regions with local stacks and correlation coefficients (equations 3–6) in the correlation gather between the receivers at x_B and x_A. Figure 7c shows the obtained correlation coefficient using $N = 21$,

which results in an estimated stationary-phase position at $x_{S^*} = 1850$ m. As shown in Figure 7d, the estimated stationary-phase position is quite stable for N varying from 11 to 35, as we observe a mean estimated position $\{x_{S^*}\}_{av} = 1819$ m with a stan-
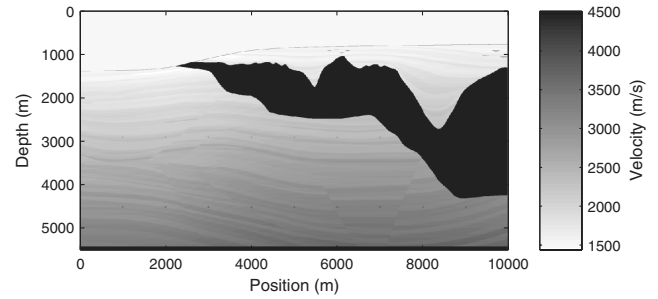

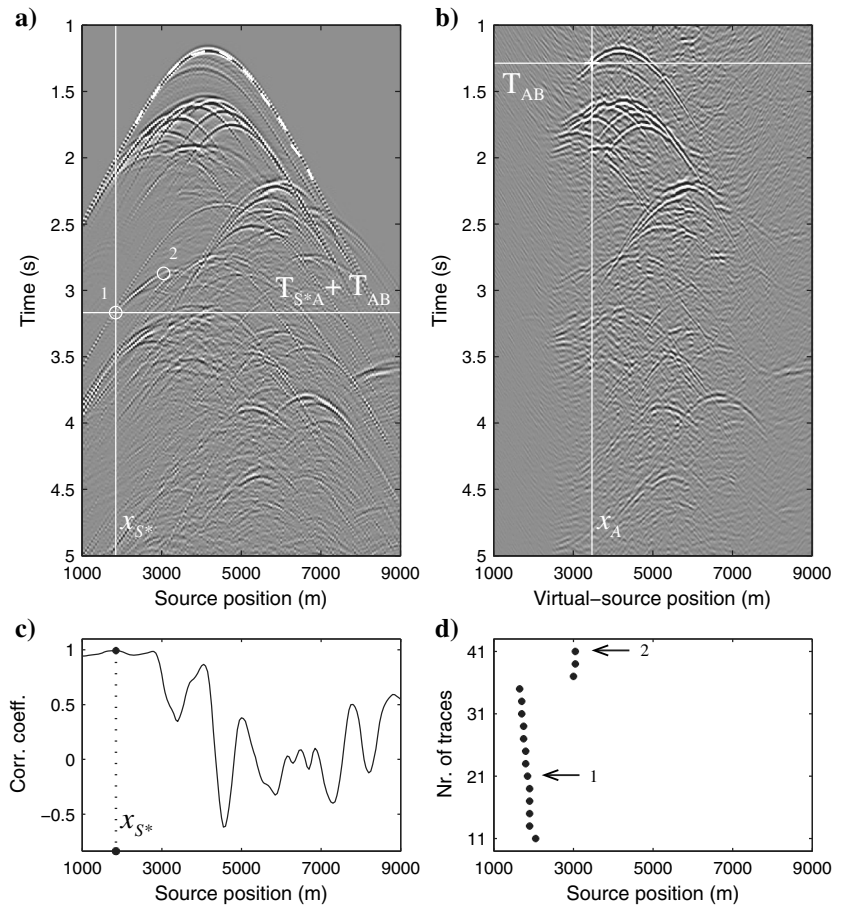Figure 6. Acoustic velocity model derived from the Sigsbee 2B model.

Figure 7. (a) Common-receiver gather for the position $x_B = 4000$ m from the modeled-reflection data. The dashed white line indicates the selected physical reflection event. (b) Common-receiver gather for the position $x_B = 4000$ m from the retrieved-virtual data. The white cross indicates the picked virtual-source position for the retrieved pseudophysical reflection event. (c) Correlation coefficient as a function of the source position with $N = 21$. (d) Detected stationary-phase source position as a function of the number of stacked adjacent traces N in equation 5. The predicted arrival time of a surface multiple for $x_{S^*} = 1850$ m ($N = 21$, index 1) is indicated in (a) by a white circle. The second white circle indicates the predicted arrival time for the detected source position $x_{S^*} = 3050$ m using $N = 41$ (index 2).

dard deviation of 110 m. The predicted arrival time of a surface multiple for $N = 21$ (index 1) is indicated by a white circle at crossing white lines in Figure 7a. Choosing any N between 11 and 35 would result in the identification of the same multiple event but at slightly shifted source positions. For the higher numbers of stacked traces ($N = 37, 39$, and 41), the stacking window exceeds the dominant stationary-phase region, which is thus not captured anymore.

As a result, another stationary-phase region is identified. Both regions contribute constructively to the retrieval of the pseudoreflection and both indicate the presence of a multiple in the original data. The predicted arrival time for $N = 41$ (index 2) is indicated with a single white circle. This result shows that rather than estimating an erroneous stationary-phase position x_{S^*}, we have detected another (with lower contribution) stationary-phase position, resulting in a
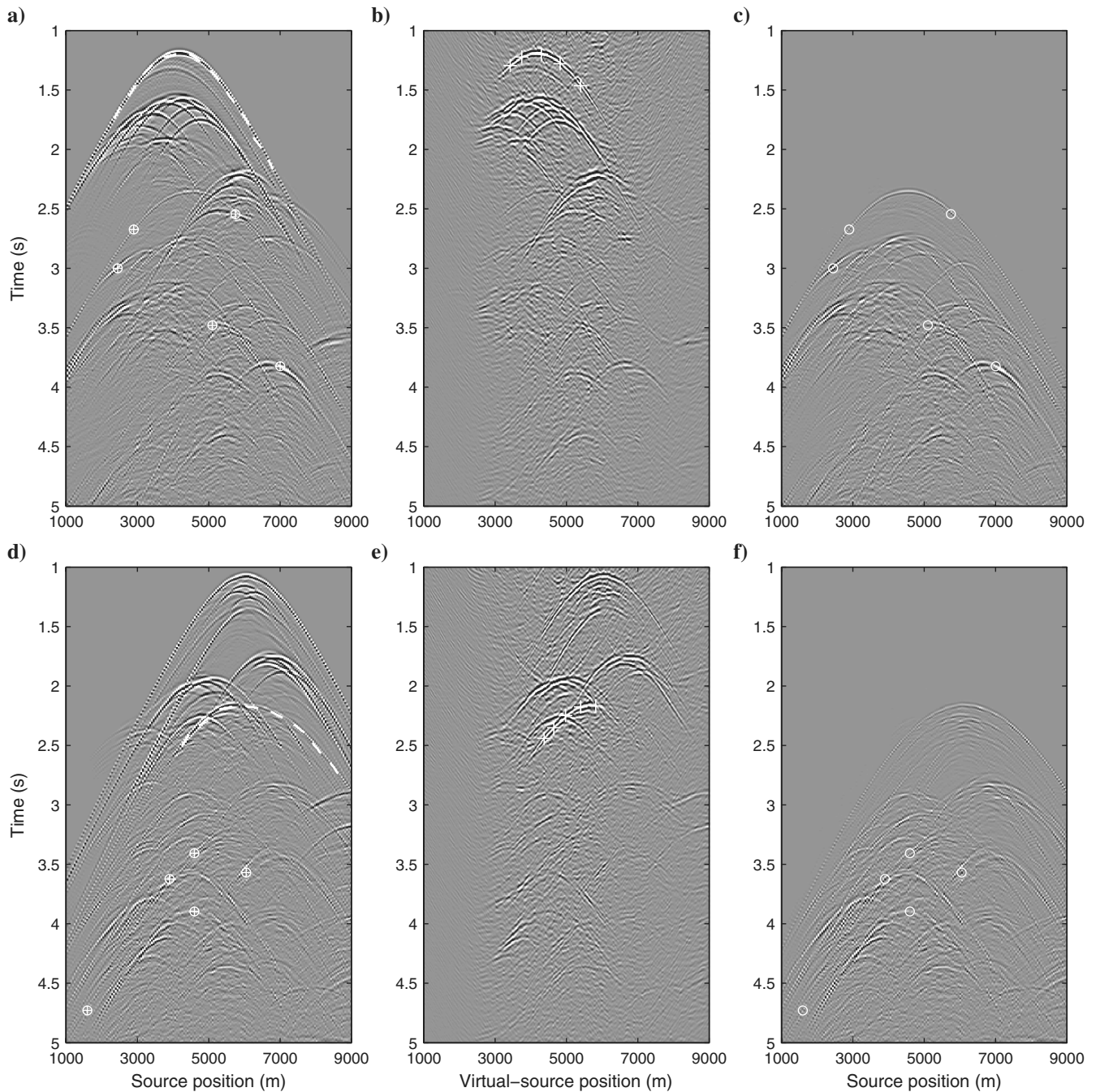

Figure 8. (a) Common-receiver gather for the position $x_B = 4000$ m from the modeled-reflection data. The dashed white line indicates the selected physical reflection event. (b) Common-receiver gather for the position $x_B = 4000$ m from the retrieved-virtual data. The white crosses indicate the picked virtual-source position for the retrieved pseudophysical reflection event. The resulting predicted arrival of multiples is marked with white circles in the gather in (a). (c) As in (a), but with suppressed primary reflections. (d-f) The identification of surface-multiple arrivals as in (a-c) but for $x_B = 6000$ m and a different selected physical reflection.

new point of identification of another multiple. Note that this second stationary-phase region was already revealed by the second-highest peak on the graph in Figure 7c obtained with $N = 21$.

We pick several arrival times along the selected pseudophysical reflection, which are depicted as white crosses in Figure 8b, thus doing the stationary-phase analysis for several virtual-source positions. The resulting predicted arrival times of surface multiples are indicated in the reflection-data gather in Figure 8a as well as in Figure 8c, in which the primaries are suppressed. The result of Figure 8c shows that strong surface multiples are correctly identified using the proposed interferometric diagnosis. Moreover, the identified multiple arrivals are localized in a large range of the gather. It is also interesting to notice that the sea-bed primary reflection is not always the main contributor to the retrieved pseudophysical reflection; also other subsurface reflectors, such as the top of the salt, are identified as significant multiple generators.

We also test the interferometric identification for the common-receiver gather for position $x_B = 6000$ m and by defining a new traveltime curve corresponding to a different (later) physical reflection (dashed white curve in Figure 8d). The resulting predictions of surface-multiples arrivals in the gather are marked with white crosses in Figure 8d as well as in Figure 8f, in which the primaries are suppressed. The result in Figure 8f shows that different strong surface multiples are again correctly identified by the method. Note that Figure 8f also reveals that the selected traveltime curve corresponds, at least partly, to a first-order surface multiple, leading to the prediction of arrival times of the second-order (and higher order) surface multiples.

The above numerical examples show that strong surface-multiple arrivals can be located in noise-free reflection data using an interferometric diagnosis. However, field data are always contaminated with random noise, such as instrument noise or ambient noise. To address the effect of noise and get closer to field data, we added random noise to the modeled reflection data. The noise follows a Gaussian distribution and is present in the same frequency band as the reflection signals (white Gaussian noise). Figure 9a shows the same common-receiver panel as in Figure 7a but with added random noise using an S/N = 8. The S/N is defined with respect to the maximum amplitude of the reflection signal in a shot gather. For this reason, a ratio of eight represents high level of noise, as visible in Figure 9a. In addition, because the noise level is constant, the effective signal-to-noise ratio decreases with time.

Next, we applied the same analysis, as described in Figure 8, to the noisy data. We apply seismic interferometry to the noisy data to retrieve virtual data (Figure 9b). Using the same selected retrieval time and virtual-source position, we estimate a stationary-phase position (Figure 9c) and locate the surface-multiple arrival in Figure 9a. This arrival coincides with identifications obtained in Figures 7a and 8a. We tested the stationary-phase detection and multiple identification for

increasing noise levels from S/N = 20 to 4. Figure 9c shows the estimated dominant stationary-phase position as a function of S/N. We observe that in any of the considered noise scenarios, the estimated position x_S^* remains within one of the two prominent stationary-phase regions identified from the noise-free data in Figure 7. Because these two regions have comparable levels of contribution, the estimation may correspond to a different region depending on the modeled noisy data. This explains, for example, the shift observed between the results for S/N = 20 and S/N = 18. The study with S/N = 8 represents a worst-case scenario in which only a few surface multiples in the data are above the noise level.

As we previously mentioned, the surface-multiple signals appear weaker as the noise level increases. Therefore, the result of the increase in noise level may also be thought of as data that have undergone a poor attenuation of multiples, i.e., that multiples have become weaker, but are still present in the data. If the weaker, but present, multiple energy remains above the noise level, then one will still retrieve pseudophysical energy and the stationary-phase analysis can be applied to locate the strongest of the contributing surface multiples.
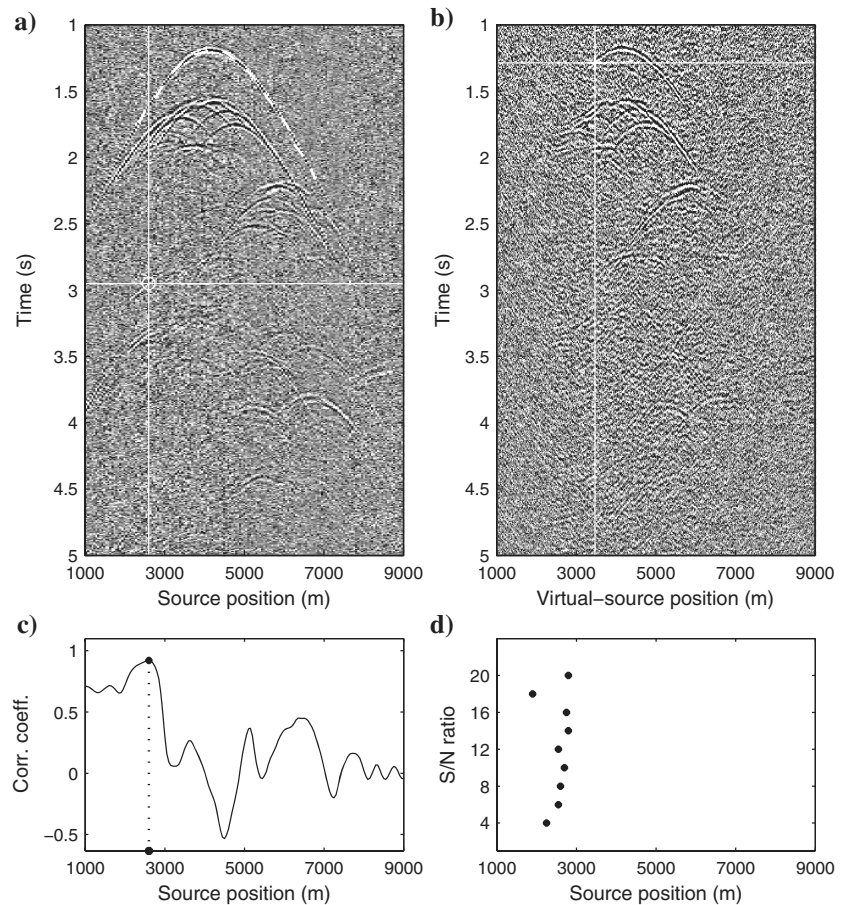

Figure 9. (a) Common-receiver gather as in Figure 7 but with added random noise (signal-to-noise ratio of 8). The dashed white line indicates the selected physical reflection event. (b) Common-receiver gather for the position $x_B = 4000$ m from the retrieved-virtual data. The white cross indicates the picked virtual-source position for the retrieved pseudophysical reflection event. (c) Correlation coefficient as a function of the source position for $N = 21$. The predicted arrival time of a surface multiple for $x_{S^*} = 2600$ m is indicated by a white circle in (a). (d) Detected stationary-phase source position as a function of the S/N.

Finally, an interesting property of the interferometric approach is that the wavefield crosscorrelation permits retrieving useful pseudophysical reflection data from reflection data without the near offsets. This property is exploited by Curry and Shan (2010) to reconstruct the missing near offsets with interferometric traces. Here, we aim to demonstrate the possibility of identifying surface multiples in reflection data with missing near offsets. Note that, with this type of data, multiple prediction by convolution-based methods may fail because of the missing near-offset recordings. For this reason, the reflection data are commonly first interpolated at the missing near offsets before multiple prediction. However, the interpolation is not necessarily trivial and the subsequent elimination of the multiples may not always be successful. An interferometric approach, as presented here, could thus be used to control the quality of the multiple eliminations, especially for data without near offsets. Figure 10a shows the common-receiver gather for position $x_B = 4000$ m, as in Figure 8a, with the nearest offsets up to 500 m missing. The reflection data with missing near offsets are used to retrieve the virtual data. Figure 10b shows retrieved receiver gather for position $x_B = 4000$ m. When compared with the gather in Figure 8b, we observe that missing the near offsets causes the signal-to-noise ratio to slightly decrease in the retrieved data. Still, retrieved pseudophysical reflections are clearly present and can be detected. We use the same traveltime curve as in Figure 8b for the detection, and we select new virtual-source positions for the detected nonphysical reflection. The resulting predicted arrival times of surface multiples are plotted in Figure 10a as well as in Figure 10c for suppressed primaries. Although near offsets were missing in the reflection data, multiples are here still identified correctly, at near (close to 500 m) and intermediate offsets. The maximum extent of the missing near offsets tolerated by the method will depend on the number of surface multiples present in the data, because using correlation we may retrieve pseudoreflections even from high-order multiples.

The offset requirements of the convolution-based methods and the interferometric approach can also be discussed in the light of the situation in Figure 2, i.e., illustratively for horizontally layered subsurface. The surface multiple from x_S to x_B, as depicted in Figure 2a, can be predicted by convolution of the primary reflection from the source at x_S to the receiver at x_A with the primary reflection from the source at x_A to the receiver at x_B. Therefore, letting D be the distance from x_S to x_B, the prediction of the surface multiple would require that the reflection data contain offsets equal to and slightly shorter than $(D/2)$ m. If these offsets are near offsets and are missing, the multiple reflections would not be predicted. Moreover, missing the near offsets may considerably affect the prediction of multiples not only for the short offsets but also for intermediate and large offsets. Using correlations through the process of seismic interferometry, the retrieved pseudophysical reflection between the two receivers at x_A and x_B is obtained from a stationary-phase source distanced by D m from x_B. This source position may then be used to predict the first-order surface multiple at the offset of D m. In addition, the stationary-phase source at an offset of $(3D/2)$ can be used to identify the second-order surface multiple at the same offset (Figure 2b). Again, in Figure 2c, the identification of the surface multiple is only permitted if a source is present at the corresponding offset. Therefore, the stationary-phase analysis should still be possible for wide-azimuth-type surveys. In general, the prediction of the arrival time of a surface multiple at an offset of D m requires having the offsets in the reflection data around D m. However, not having these offsets will not significantly affect the interferometric identification of surface multiples at offsets larger than D m. Therefore, the convolution method is more dependent on having the near-offset reflection data than the crosscorrelation approach. Note, however, that the interferometric identification of surface multiples at the longest offsets is limited by the lack of sources for
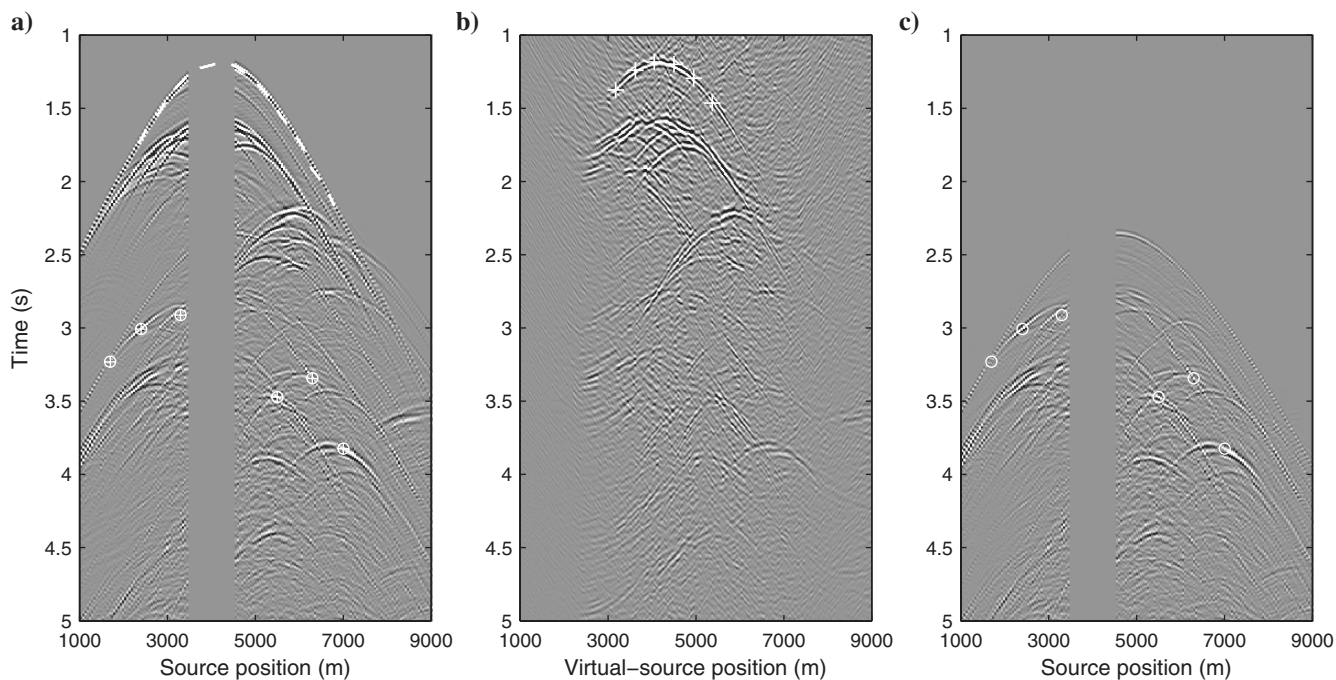

Figure 10. (a-c) As in Figure 8a–8c, but with the reflection data missing the nearest offsets up to 500 m and selecting different virtual-source positions in (b).

a proper interferometric stack. In this respect, convolutions and crosscorrelation approaches might prove to be complementary.

DISCUSSION

As mentioned above, applying seismic interferometry to surface reflection data retrieves nonphysical reflections (see, e.g., Figure 3b). These retrieved events, also known as "spurious" or "ghost" reflections, are basically virtual intralayer(s) reflections (as if the acquisition level coincides with a subsurface interface), which result largely, but not only, from the crosscorrelation of different primary events. Therefore, although strongly velocity-dependent, the nonphysical reflections may exhibit strong amplitudes, especially at the earlier times. In addition, they may have kinematics close to those of actual reflections, and can thus be confused with retrieved pseudo-primaries. In some cases, the nonphysical reflections might even interfere with arrivals of pseudophysical reflections. We expect that, for such cases, selecting retrieved events for diagnosis within the interference zone may lead to the detection of stationary-phase sources for the retrieved nonphysical reflection instead of for the pseudophysical reflection, thus resulting in erroneous predicted arrival times of surface multiples. In the scheme presented above, we partially solve this issue by using a detection threshold for the signal-to-noise ratio observed in the retrieved data along the selected traveltime curve from the reflection data. In this way, we aim to reject the use of pseudoreflection arrivals that are contaminated with noise (including spurious reflection arrivals) for multiple diagnosis. Note that several nonphysical reflections might be easily isolated, as in the situation of Figure 3b because of their kinematics. Moreover, further identification might be achieved using source-receiver interferometry, as in King and Curtis (2012) or as in Draganov et al. (2012) using velocity information, for example, from VSP data.

Because any retrieved pseudophysical reflection (primary or multiple) may be used for the interferometric diagnosis, the method can be made event-oriented. As could be seen from the examples, using one selected pseudophysical reflection could result in identified points pertaining to different multiples. This comes from our current implementation of the stationary-phase analysis, which determines only the maximal contribution, and also due to the subsurface model (impedance contrasts and complexity). Thus, for a given retrieved pseudophysical reflection arrival, once a stationary-phase source is detected, we do not make any direct assumption about the corresponding contributor. Instead, we determine the reflection event associated with that stationary-phase source by finding the strongest correlated event along the stationary travel path (Figure 4a–4c). The reason is that the contributing reflection event recorded at the virtual-source position must depend on the estimated stationary-phase position to provide a consistent arrival-time estimate of a surface multiple. Interestingly, the results in Figures 4g and 7a show that surface multiples can be identified in several points due to different stationary-phase sources detected. This suggests that a single correlation gather can be exploited beyond our current stationary-phase analysis, which estimates only the most contributing source position. Indeed, the stationary-phase analysis could be modified to estimate several stationary-phase source positions at once (thus including those from weaker contributions) to obtain more identification points in the reflection data using the same receiver pair in the retrieved data. We expect this future work to be possible as long as the different stationary-phase regions have sufficient spatial separation.

The identification method we propose allows the sources and receiver to have irregular sampling. The receiver grid does not need to be regular for the application of seismic interferometry because summation takes place only over sources. However, the interferometric retrieval, as defined in equation 2, does require a regular source sampling. Yet, it is possible to deal with irregular source grids by applying weights in the summation process (Ruigrok et al., 2010). Note that the retrieval of pseudoreflections requires the source sampling to obey the Nyquist criterion, at least around the stationary-phase regions of interest. The method also allows, to some extent, the sources and receivers to be on different grids. The only limitation is that their positions remain in the same range because, to detect retrieved pseudoreflections, we compare common-receiver gathers from the original data (varying source position) with those retrieved in the virtual data (varying virtual-source [receiver] position).

Finally, extension of the method to 3D is straightforward as long as the source coverage is sufficient to retrieve useful pseudophysical reflections and capture stationary-phase regions. In addition, a 3D acquisition geometry may circumvent the need for good, regular sampling inline with the receivers. Active sources situated in the crossline direction, but laying close to the line (in a wavelength sense) would still contribute to the retrieval of pseudophysical reflections in the inline direction.

CONCLUSION

Surface-related multiples are useful seismic signals for applications of seismic interferometry to surface reflection data. Their crosscorrelation with primary reflections and lower order surface multiples allows retrieving pseudophysical reflections in the virtual interferometric data. These interreceiver virtual events are recognized because they share the same kinematics as recorded reflections (including multiple reflections) and, in turn, can be exploited as feedback for the presence of surface multiples. Therefore, based on the stationary-phase analysis of the retrieved pseudophysical reflections, we introduce a method to detect and identify prominent surface-related multiples in the original reflection data. We exploit the correlation gathers between pairs of receivers to determine prominent secondary stationary-phase source positions, which we use in turn to estimate the arrival times of corresponding surface multiples in the reflection data. For our method, the source and receiver positions are not required to be on the same grid, as for regularized data. Although the interferometric method we propose is not a full multiple-prediction method, our tests on modeled reflection data show that the arrival times of strong multiples can be predicted with good accuracy in a large range of the data. In addition, the multiple identification still performs well with reflection data without the near offsets. Accordingly, complementary identification can be provided to convolution-based prediction methods suffering from missing near offsets. Therefore, the proposed interferometric identification could be used for quality control of conventional multiple-elimination schemes, by detecting and localizing in the reflection data leaking energy from surface-related multiples.

ACKNOWLEDGMENTS

REFERENCES

Bakulin, A., and R. Calvert, 2006, The virtual-source method: Theory and case study: Geophysics, **71**, no. 4, SI139–SI150, doi: 10.1190/1.2216190.

Berkhout, A. J., and D. J. Verschuur, 1997, Estimation of multiple scattering by iterative inversion. Part I: Theoretical considerations: Geophysics, **62**, 1586–1595, doi: 10.1190/1.1444261.

Berkhout, A. J., and D. J. Verschuur, 2006, Imaging of multiple reflections: Geophysics, **71**, no. 4, SI209–SI220, doi: 10.1190/1.2215359.

Bharadwaj, P., G. Schuster, I. Mallinson, and W. Dai, 2012, Theory of super-virtual refraction interferometry: Geophysical Journal International, **188**, 263–273, doi: 10.1111/j.1365-246X.2011.05253.x.

Boullenger, B., A. Verdel, B. Paap, J. Thorbecke, and D. Draganov, 2015, Studying CO_2-storage with ambient-noise seismic interferometry: A combined numerical feasibility study and field-data example for Ketzin, Germany: Geophysics, **80**, no. 1, Q1–Q13, doi: 10.1190/geo2014-0181.1.

Boullenger, B., K. Wapenaar, and D. Draganov, 2014, A method to suppress spurious multiples in virtual-source gathers retrieved using seismic interferometry with reflection data: 84th Annual International Meeting, SEG, Expanded Abstracts, 4087–4091, doi: 10.1190/segam2014-1107.1.

Campillo, M., and A. Paul, 2003, Long-range correlations in the diffuse seismic coda: Science, **299**, 547–549, doi: 10.1126/science.1078551.

Claerbout, J. F., 1976, Fundamentals of geophysical data processing: Blackwell Scientific Publications.

Curry, W., and G. Shan, 2010, Interpolation of near offsets using multiples and prediction-error filters: Geophysics, **75**, no. 6, WB153–WB164, doi: 10.1190/1.3506557.

Dong, S., J. Sheng, and G. T. Schuster, 2006, Theory and practice of refraction interferometry: 76th Annual International Meeting, SEG, Expanded Abstracts, 3021–3024, doi: 10.1190/1.2370154.

Draganov, D., X. Campman, J. Thorbecke, A. Verdel, and K. Wapenaar, 2009, Reflection images from ambient seismic noise: Geophysics, **74**, no. 5, A63–A67, doi: 10.1190/1.3193529.

Draganov, D., K. Heller, and R. Ghose, 2012, Monitoring CO_2 storage using ghost reflections retrieved from seismic interferometry: International Journal of Greenhouse Gas Control, **11**, S35–S46, doi: 10.1016/j.ijggc.2012.07.026.

Halliday, D. F., A. Curtis, J. O. A. Robertsson, and D.-J. van Manen, 2007, Interferometric surface-wave isolation and removal: Geophysics, **72**, no. 5, A69–A73, doi: 10.1190/1.2761967.

Hampson, D., 1986, Inverse velocity stacking for multiple elimination: Journal of the Canadian Society of Exploration Geophysicists, **22**, 44–55.

Kelamis, P. G., and D. J. Verschuur, 2000, Surface-related multiple elimination on land seismic data: Strategies via case studies: Geophysics, **65**, 719–734, doi: 10.1190/1.1444771.

King, S., and A. Curtis, 2012, Suppressing nonphysical reflections in Green's function estimates using source-receiver interferometry: Geophysics, **77**, no. 1, Q15–Q25, doi: 10.1190/geo2011-0300.1.

Löer, K., G. Meles, A. Curtis, and I. Vasconcelos, 2013, Diffracted and pseudo-physical waves from spatially-limited arrays using source-receiver interferometry (SRI): Geophysical Journal International, **196**, 1043–1059, doi: 10.1093/gji/ggt435.

Mikesell, D., K. van Wijk, A. Calvert, and M. Haney, 2009, Virtual refraction: Useful spurious energy in seismic interferometry: Geophysics, **74**, no. 3, A13–A17, doi: 10.1190/1.3095659.

Ruigrok, E., X. Campman, D. Draganov, and K. Wapenaar, 2010, High-resolution lithospheric imaging with seismic interferometry: Geophysical Journal International, **183**, 339–357, doi: 10.1111/j.1365-246X.2010.04724.x.

Ruigrok, E., and K. Wapenaar, 2012, Global-phase seismic interferometry unveils P-wave reflectivity below the Himalayas and Tibet: Geophysical Research Letters, **39**, L11303, doi: 10.1029/2012GL051672.

Sabra, K. G., P. Gerstoft, P. Roux, W. A. Kuperman, and M. C. Fehler, 2005, Extracting time-domain Green's function estimates from ambient seismic noise: Geophysical Research Letters, **32**, L03310, doi: 10.1029/2004GL021862.

Schuster, G. T., 2009, Seismic interferometry: Cambridge University Press.

Schuster, G. T., J. Yu, J. Sheng, and J. Rickett, 2004, Interferometric/daylight seismic imaging: Geophysical Journal International, **157**, 838–852, doi: 10.1111/j.1365-246X.2004.02251.x.

Schuster, G. T., and M. Zhou, 2006, A theoretical overview of model-based and correlation-based redatuming methods: Geophysics, **71**, no. 4, SI103–SI110, doi: 10.1190/1.2208967.

Snieder, R., 2004, Extracting the Green's function from the correlation of coda waves: A derivation based on stationary phase: Physical Review E, **69**, 046610, doi: 10.1103/PhysRevE.69.046610.

Snieder, R., K. Wapenaar, and K. Larner, 2006, Spurious multiples in seismic interferometry of primaries: Geophysics, **71**, no. 4, SI111–SI124, doi: 10.1190/1.2211507.

Trad, D., 2003, Interpolation and multiple attenuation with migration operators: Geophysics, **68**, 2043–2054, doi: 10.1190/1.1635058.

van Borselen, R. G., J. T. Fokkema, and P. M. van der Berg, 1996, Removal of surface-related wave phenomena: The marine case: Geophysics, **61**, 202–210, doi: 10.1190/1.1443940.

van Groenestijn, G. J. A., and D. J. Verschuur, 2009, Estimating primaries by sparse inversion and application to near-offset data reconstruction: Geophysics, **74**, no. 3, A23–A28, doi: 10.1190/1.3111115.

van Wijk, K., 2006, On estimating the impulse response between receivers in a controlled ultrasonic experiment: Geophysics, **71**, no. 4, SI79–SI84, doi: 10.1190/1.2215360.

Verschuur, D. J., A. J. Berkhout, and C. P. A. Wapenaar, 1992, Adaptive surface-related multiple elimination: Geophysics, **57**, 1166–1177, doi: 10.1190/1.1443330.

Wapenaar, K., 2004, Retrieving the elastodynamic Green's function of an arbitrary inhomogeneous medium by cross correlation: Physical Review Letters, **93**, 254–301, doi: 10.1103/PhysRevLett.93.254301.

Wapenaar, K., and J. Fokkema, 2006, Green's function representations for seismic interferometry: Geophysics, **71**, no. 4, SI33–SI46, doi: 10.1190/1.2213955.

Yilmaz, O., 1987, Seismic data processing: SEG.